J Polym Res (2007) 14:467–474
DOI 10.1007/s10965-007-9130-x

Characterization on oxidative stabilization of polyacrylonitrile nanofibers prepared by electrospinning

Wang-xi Zhang · Yan-zhi Wang · Chun-feng Sun

Received: 21 February 2007 / Accepted: 19 June 2007 / Published online: 21 July 2007

Abstract Ultrafine polyacrylonitrile (PAN) fibers, as a precursor of carbon nanofibers, with diameters in the range of 220–760 nm were obtained by electrospinning of PAN solution using *N*,*N*-dimethyl formamide (DMF) as solvent. Morphology of the nanofibers for varying concentration and applied voltage was investigated by field emission scanning electron microscopy (FESEM). The thermal properties and structural changes during the oxidative stabilization process were primarily investigated by differential scanning calorimetry (DSC), thermogravimetric analysis (TGA), and Fourier transform infrared (FT-IR) and Raman spectroscopy. The nanofiber diameters increase as the applied voltage is increased and they also increase with an increase in the concentration of the polymer solution. It was also concluded that the electrospun fibers displayed a very sharp exothermic peak at 297.34 °C. A transition temperature observed by FT-IR and Raman was approximately 300 °C, which was closely consistent with the results of DSC and TGA studies. It was also found that oxidative stabilization in air was accompanied by a change in color of nanofibers webs.

Keywords Electrospinning · Oxidative stabilization · Polyacrylonitrile · Nanofibers

W.-x. Zhang (✉) · Y.-z. Wang
School of Materials & Chemical Engineering,
Zhongyuan University of Technology,
Zhengzhou 451191, China
e-mail: wangxizhang.zheng@yahoo.com.cn

C.-f. Sun
Department of Resources & Environmental Engineering,
North China Institute of Science & Technology,
Beijing 101601, China

Introduction

Various polymer solutions or melts [1], composites [2], and sol–gel ceramics [3] have been successfully electrospun into nanoscale, or ultrafine fibers by the use of electrospinning which has been commonly accepted in the past few years on account of the remarkable simplicity, versatility, and potential uses of this approach. Although electrospinning has not been widely used in an industrial scale at present, tremendous progress has been made to improve the related equipment and processes. Kim et al. [4] introduced a modified electrospinning process to improve the mass productivity of multi-nozzle electrospinning, using an auxiliary electrode for increasing the production rate of nanofibers manufacturing. Bead formation should be avoided as possible according to the results of Fong et al. [5]. Ali and Hamid [6] studied the optimization of some electrospinning parameters, such as spinning angles, charge density, etc. for preparing a precursor of carbon nanofibers. For many applications, it is critical to control the alignment of the fibers. Electrospinning fibers, however, are often collected in the form of randomly oriented, non-woven fabrics. Some research groups have demonstrated the ability to directly collect electrospun nanofibers as uniaxially aligned arrays by the use of a rotating drum [7] or a pair of split electrodes as the collector [8]. Smit et al. [9] also obtained continuous uniaxial fiber bundle yarns by electrospinning onto a water bath collector followed by a take-up roller.

Nanofibers are expected to be used in various fields, such as catalysis [10], scaffolds for tissue engineering [11], drug delivery systems [12, 13], antibacterial agents [14], super-paramagnetic field-responsive materials, filtration, wound dressings, and so on. Potential applications of electrospun nanofibers in energy generation, defense and security, biotechnology and environmental engineering, and healthcare have been reviewed in detail by Ramakrishna et al. [15]. Conductive nanofibers or webs have potential for applications in the fabrication of tiny electronic devices. Fundamental studies have demonstrated that carbon nanofibers possess an unusual combination of properties that include high mechanical properties, high surface area and high electrical conductivity. It is well-known that nanoscale or ultrafine polyacrylonitrile(PAN) precursors can be transformed into conductive carbon nanofibers, [16] which can be used to produce carbon–carbon nanocomposite fibrils with carbon nanotubes [17, 18], or to be an ideal candidate for the anode material of high-power lithium-ion batteries. Carbon nanofibers are also finding applications in unconventional energy sources and storage cells, and synthetic and rubber industries [19].

To prepare traditional polyacrylonitrile-based carbon fibers in mass scale, three key steps are necessary including (1) spinning a polymer into fibers; (2) an oxidative stabilization process, also named as preoxidation at 200–300 °C under air atmosphere; (3) a carbonization process performed at 400–1,400 °C commonly under nitrogen atmosphere, sometimes in argon gas. The same is true of electrospun nanofibers of PAN. The oxidative stabilization is a time-consuming and reaction-controlling step during the conversion of fiber precursors to resulting carbon fibers and should be optimized in order to improve the final mechanical properties of carbon fibers. A radical reaction mechanism for a PAN homo-polymer precursor and an ionic reaction mechanism for one originating from copolymers of acrylonitrile and itaconic acid, acrylamide, etc. [20] were put forward. Sutasinpromprae et al. [21] reported the fabrication and characterization of ultrafine PAN fibers by electrospinning and further development of the as-spun fibers into ultrafine carbon fibers. They also investigated the effects of solution conditions (i.e., solution concentration, viscosity, conductivity, and surface tension) and process parameters (i.e., applied electrostatic field strength, emitting electrode polarity, nozzle diameter, and take-up speed of a rotating-drum collector) on morphological appearance and average diameter of the as-spun PAN fibers. Kim et al. [22] and Wang et al. [23] reported Raman spectroscopic evaluation of PAN-based carbon nanofibers prepared using electrospinning.

Oxidative stabilization is considered to be the most decisive step, and it is also of the utmost importance in industrial fabrications, since it significantly governs the final structure and ultimate mechanical properties of the carbon fibers [24]. However, few studies on the oxidative stabilization of electrospun PAN fibers have been undertaken. In the present contribution, PAN homopolymers were electrospun into ultrafine nanofibers. The effects of solution concentration and applied voltage on the morphology and sizes of nanofibers were of primary concern. The thermal properties related to heat treatment and structural changes of nanofibers during the process of oxidative stabilization performed at 250–310 °C in air were in investigated detail.

Experimental

Materials

Polyacrylonitrile(PAN) (Product Number 18,131-5) with 150,000 weight average molecular weight was obtained from Sigma-Aldrich. The 99% *N*,*N*-Dimethylformamide (DMF) (Product Number D158,550) was also purchased from Sigma-Aldrich and used without further purification. A predetermined amount of PAN was added to DMF at room temperature, oscillating for 2 h in an incubator, followed by stirring using a magnetic stirring apparatus at 60 °C for 6 h to obtain a homogenous polymer solution with concentration of 8 wt.% (by weight), 10 wt.%, or 12 wt.%, to be used to obtain nanofibers using electrospinning. For comparison, a PAN film was also cast from a 10 wt.% PAN/DMF solution and dried in a vacuum oven.

Electrospinning of nanofibers and their oxidative stabilization

For a typical electrospinning procedure, a PAN/DMF polymer solution was loaded into a 20 ml plastic syringe equipped with a 0.8 mm (inner diameter) and 1.1 mm (outer diameter) gauge needle made of stainless steel. The needle was connected to a high-voltage supply (PS/FC30R04.0-22, Glassman High Voltage, UK) that is capable of generating direct current (DC) voltages up to 22 kV. The solution was constantly and controllably supplied using a syringe pump (SP230IWZ Syringe Pump, USA) at a flow rate of 0.5 or 1 ml h^{-1}. A flat metal plate with aluminum foil placed below served as a grounded counter electrode. In this study, the grounded targets were always placed at 10 cm (tip-to-collector) from the needle tip. The fibers were collected on the aluminum foil in the form of non-woven fabric.

The as-spun nanofibers were heated from room temperature at a heating rate of 1 °C min^{-1} to heat treatment temperatures (HTT) at 250, 280, 300, 310 °C, respectively, by using a Carbolite ESF 12/10 muffle furnace (made in U.K.). After reaching the specified temperature, the fibers were oxidatively stabilized without being stretched for predetermined times in air. For the aim of comparison, the fibers as-stabilized at 310 °C were subsequently carbonized by heating at a heating rate of 2 °C min in Argon gas by use of the Carbolite tube furnace.

Differential scanning calorimetry (DSC) and thermogravimetric analysis (TGA)

The exothermic reaction of electrospun PAN precursor fibers was determined by the use of DSC which was carried out on a DSC-Q100 module of a TA instruments (USA). These DSC studies were performed at a heating rate of 10 °C in nitrogen atmosphere with sample weights of about 5 mg. The thermal stability of the electrospun fibers were also measured by thermogravimetric analysis (TGA) with samples of 1.3 mg using a Hi-Res Modulated TGA 2950 TA Instruments up to 800 °C at a heating rate of 10 °C min^{-1} in N_2.

Fourier transform infrared spectroscopy

Fourier transform infrared (FT-IR) spectra were obtained by the use of a NICOLET 5700 FT-IR Microscope (USA).

Scanning electron microscope (SEM)

The as-electrospun fibers were observed in a Philips XL30 FEG field emission scanning electron microscopy (FESEM) with operating voltage of 2 kV. Samples were mounted onto SEM plates and sputter coated with gold to examine the morphological appearance and size of fibers. In order to obtain the diameter of the fibers, at least 50 readings were recorded, from which an arithmetic mean and a standard deviation were obtained.

Raman spectroscopy

The Raman spectra were obtained using a Renishaw 1000 Raman microprobe system and were excited using the 514.5 nm green line of a 10 mW argon ion laser under ambient conditions with exposure time of 30 s and accumulating 2 times. The microscope used a 50-time objective lens to focus the laser beam on the sample surface.

Results and discussion

The morphology of electro-spun PAN precursors

In the electrospinning process, when the electric force on induced charges on the polymer liquid overcomes surface tension, a thin polymer jet is ejected [25].The polymer jet thinning trajectory is in a very complicated three-dimensional “whipping” way, caused by bending instability, rather than in a straight line [26].There are three kinds of instability modes during the process of electrospinning: Rayleigh instability, axisymmetric instability, and whipping instability [27]. Which instability dominates depends strongly on the surface charge density and radius of the jet. However, the properties of the solution, such as concentration and viscosity, as well as applied voltage and tip-to-collector distance may be adjusted in order to obtain a stable jet.

Figure 1 shows some selected FESEM images of as-electrospun nanofibers with varying applied voltages. The diameters of as-electrospun PAN fibers at various applied voltage are listed in Table 1. In this study, the diameters of the as-spun fibers increase as the applied voltage is increased. This is the reason that the increase of applied voltages will result in an increase in the electrostatic force acting on an infinitesimal segment of an ejected, charged jet, which may result in an increase in the mass throughput of the polymer solution to cause the initial increase in the fiber size [13]. However, if applied voltage is too high, for example, higher than 20 kV, it may possibly cause multiple jets, which will result in not only clogging or splitting because of large instability but also final variances in fiber diameters. It was also noted that some beaded, or other abnormal-shape fibers, such as dumbbell or shuttle ones, were found for electrospinning with a high applied voltage of 20 kV, as shown in Fig. 1e and f.

In the electrospinning process, different results concerning the relationships between the as-spun fiber diameters and the applied voltage were concluded. Some researchers found that the diameters of as-spun PAN fibers increase with increasing applied voltage. Ashraf and Hamid [6] found that the optimum charge density was 2.5 kV/cm and, then further increasing the charge density would increase the fiber diameter. In the report of Deitzel et al. [28], increasing the voltage causes the rate at which solution is removed from the capillary tip to exceed the rate of delivery of solution to the tip needed to maintain the conical shape of the surface. This shift in the mass balance would increase instability of the jet at the spinning tip and the fiber bead density. Our observation is in qualitative agreement with these results. On the other hand, some researchers concluded that the diameters of as-spun PAN fibers decrease with increasing applied voltage. In the studies by Kalayci et al. [29], by Fennessey and Farris [30], and by Kedem et al. [31], the fiber diameter decreased with applied voltage, which creates a stronger electric force drawing and thinning the fibers. Wang and Kumar [32] varied charge density by increasing the voltage from 13 to 27 kV while keeping the tip-to-collector distance constant at 10 cm. They reported that the fiber diameters decreased with increasing applied voltage, or the fiber diameters did not exhibit a significant dependence on applied voltage for all given solution concentration conditions. Gu et al. [33] also found that the diameter of electrospun PAN fibers did not change significantly over the range of applied voltage for the various solution concentrations. Varaporn et al. [13] reported the as-spun fibers diameters initially increased, reached a maximum value, and then decreased with increasing applied voltage.

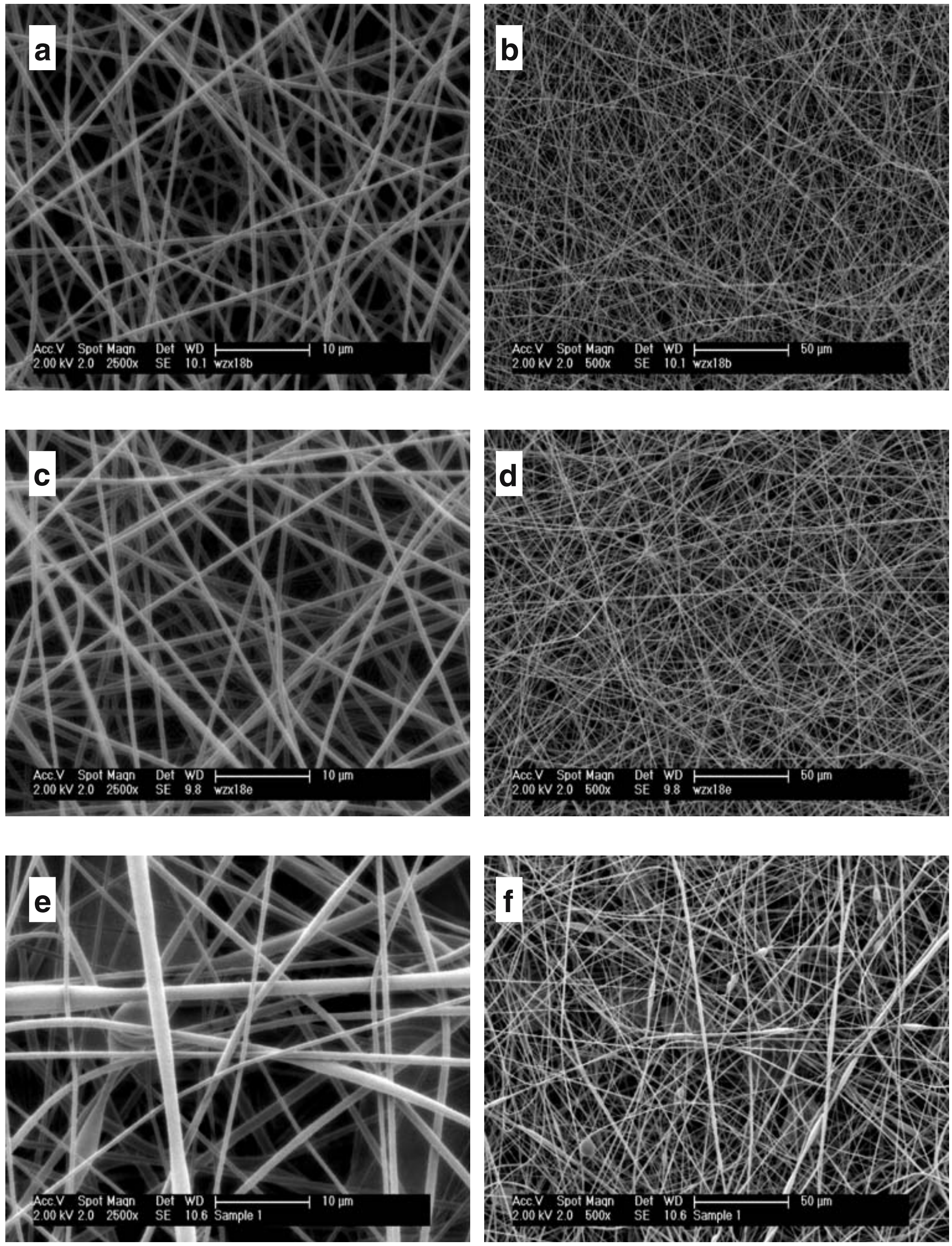

Fig. 1 Selected FESEM images of electrospun PAN fibers resulting from different applied voltages: 10 kV (**a**, **b**); 15 kV (**c**, **d**); and 20 kV (**e**, **f**). Electrospinning conditions: polymer solution concentration, 10 wt.%; flow rate, 1 ml h^{-1}; tip-to-collector, 10 cm

The inconsistency might be due to the difference of the experimental conditions. Whether or not the fibers size should increase or decrease with increasing applied voltage depends very much on the ability of the system to supply the polymer solution from the reservoir to the opening of the needle as well as the viscosity. If the flow rate was much less than the rate at which the electrostatic stress tries to pull the charged jet towards the target, the final fiber diameters should decrease. In our study, it was confirmed that the diameters of the as-spun fibers increase with increasing the applied voltage. However, if the applied voltage was higher than 20 kV, highly unstable streams whipped around in different directions, thus resulting in significantly larger differences in fiber diameters.

Figure 2 shows some selected FESEM images of as-spun nanofibers with varying the concentration of PAN/DMF solutions. Table 2 is the diameter values of as-electrospun PAN fibers at various polymer solution concentrations. It is demonstrated that the fiber's diameter increases as the concentration of the polymer solution increases. This is because of the increase in volume percent of solid in the solution and viscosity as a result of increased solution concentration with keeping other parameters unchanged. It was also seen that by using lower concentration, regardless of the electrospinning voltage, the polymer solution did not form nanofibers but fine droplets were liable to form, falling on the collecting target.

Table 1 Diameters of as-electrospun PAN fibers at various applied voltages

Applied voltage (kV)	10	15	20
Diameter (nm)	495±50	535±60	760±120

Electrospinning conditions: polymer solution concentration, 10 wt.%; flow rate, 1 ml h^{-1}; tip-to-collector, 10 cm.

Table 2 Diameters of as-electrospun PAN fibers at various polymer solution concentrations

Polymer solution concentration (wt.%)	8	10	12
Diameter (nm)	220±35	495±50	620±80

Electrospinning conditions: applied voltage, 10 kV; flow rate, 1 ml h^{-1}; tip-to-collector, 10 cm.

Thermal properties of electrospun PAN precursors

It is necessary to acquire information about the thermal properties of precursor fibers before heat treatment to transform to carbon fibers. Here, DSC curves were obtained in nitrogen atmosphere, as shown in Fig. 3. The electrospun fibers and PAN film display very sharp exothermic peaks at 297.34 °C and 296.48 °C, respectively, which is in excellent agreement with the DSC pattern of a typical PAN homopolymer [34]. The peak is regarded as the result of cyclization of the nitrile groups of PAN, which corresponds to the oxidative stabilization process; further heated at higher carbonization temperature results in transforming to the graphite-sheet-like ladder structure of carbon fibers. Gu et al. [35] compared the difference of DSC thermograms between the elcetrospun PAN fibers and a cast film originated from identical PAN resin. They found that the peak shifted to lower temperature for electrospun fibers as compared to that of cast film. In this study, however, there are no notable peak shifts between the DSC curve of electro-spun PAN fibers and that of the corresponding PAN films. The reason for this is not very clear yet. A possible explanation is that there is no notable increase in the crystallinity degree and/or orientation index for electrospun jet fibers, as a result of, that molecular chains are not rearranged regularly within the electrospun fibers during the high speed electrospinning process.

Figure 4 shows TGA curves of the electro-spun PAN fibers using a heating rate of 10 °C min^{-1} in the temperature range from room temperature to 800 °C. A slight loss of mass took place from about 95 to 120 °C due to the release of water. The main mass loss from 280 to 330 °C, attributed to the pyrolysis of the fibers, was in agreement with the peak on the DSC curve of electrospun PAN fibers; the loss slowed down above 330 °C to give a yield of 41% at 800 °C. TGA

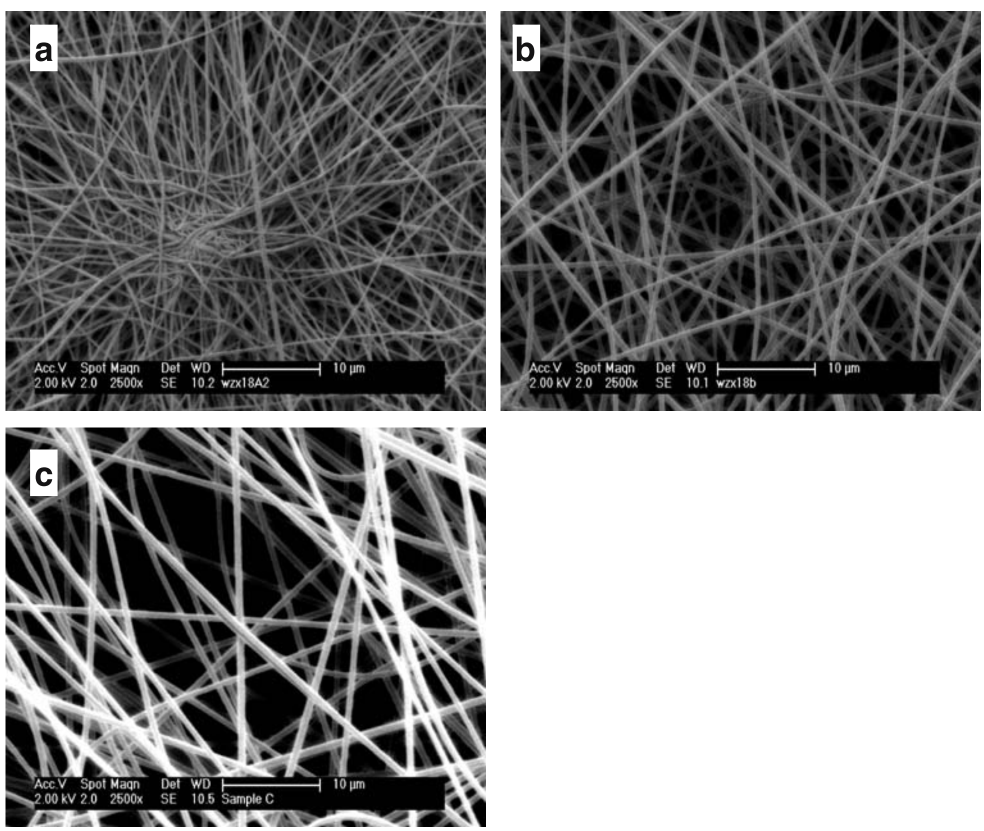

Fig. 2 Selected FESEM images of electrospun PAN fibers resulting from polymer solution concentrations 8 wt.% (**a**); 10 wt.% (**b**); and 12 wt.% (**c**). Electrospinning conditions: applied voltage, 10 kV; flow rate, 1 ml h^{-1}; tip-to-collector, 10 cm

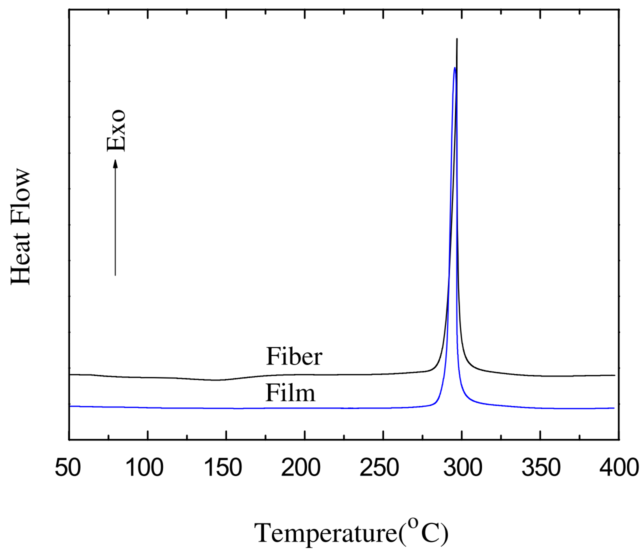

Fig. 3 The DSC thermograms of PAN film and electrospun precursor fibers

can be utilized to determine the starting temperature of oxidative stabilization and carbonization of fibers.

Changes in structure and morphology of nanofibers

When PAN nanofibers were heated in the presence of oxygen, the resulting ladder structures formed in the polymers caused the initial changes in color of nanofibers webs. As shown in Fig. 5, oxidative stabilization in air is accompanied by a change in color from white to reddish-brown, tan in the end. Furthermore, when the as-stabilized fibers were carbonized at elevated temperature, up to 450 °C in Argon gas, a dark brown nanofibers web was obtained. These molecular structure changes in the nanofibers can be further confirmed by the following FT-IR and Raman studies.

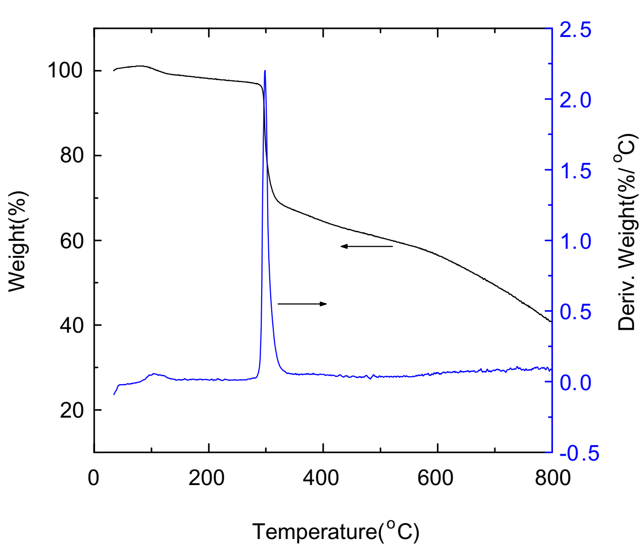

Fig. 4 The TGA curves of electrospun PAN precursor fibers

Figure 6 shows the FT-IR spectra of PAN nanofibers after different heat treatment temperature (HTT) and time. The vibrations characteristic of PAN structure are those of CN nitrile group at approximately 2,243–2,241 cm^{-1}, and the bands in the regions 2,931–2,870, 1,460–1,450, 1,380–1,350, and 1,270–1,220 cm^{-1} which are assigned to the aliphatic CH group vibrations of different modes in CH and CH_2 [36].

As the HTT is increased, the most prominent structural changes were the decrease in the intensities of the 2,243–2,241 cm^{-1}, attributed to C≡N band, and the decrease of those for aliphatic C–H ones, respectively, concomitant with the advent and increase of a shoulder-like peak at 1,700 cm^{-1}(due to cyclic C=O), the band at 1,590 cm^{-1}(due to C=N, C=C, N=H mixed), and the band at 810 cm^{-1}(due to C=C=H) [37]. These spectroscopic results show that some chemical processes occurred during the stages of oxidative stabilization, which is also in excellent agreement with those changes in PAN fibers prepared by a traditional wet, dry, or dry–wet spinning approach. [34] Firstly, reaction of nitriles results in conjugated C=N containing structures which result from intramolecular cyclization or intermolecular crosslinking. Secondly, the generation of conjugated C=C structures results from dehydrogenation or from imine–enamine tautomerization and subsequent isomerization [38]. Thirdly, oxidation gives rise to carbonyl groups. In addition, the transition temperature, approximately 300 °C, displayed in the structural changes from FT-IR spectra, is consistent with the results of our DSC and TGA studies.

To analyze the microstructure, Raman spectroscopy has been used because it is very sensitive to subtle variations in the structure of carbon-based materials which can not be characterized by FT-IR when their precursors are heated to

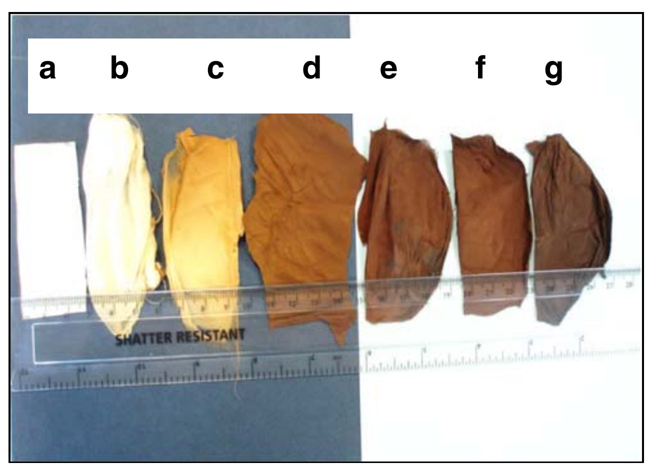

Fig. 5 Photographs of nanofibers webs: **a** electrospun as-spun fibers web (*white*), **b** as-stabilized fibers web (*buff*) (250 °C, 30 min in air), **c** as-stabilized fibers web (*yellow*) (280 °C, 30 min in air), **d** as-stabilized fibers web (*reddish-brown*) (300 °C, 30 min in air), **e** as-stabilized fibers web (*brown*) (300 °C, 120 min in air), **f** as-stabilized fibers web (*tan*) (310 °C, 120 min in air), **g** as-carbonized fibers web (*dark brown*) (450 °C, 120 min in argon gas)

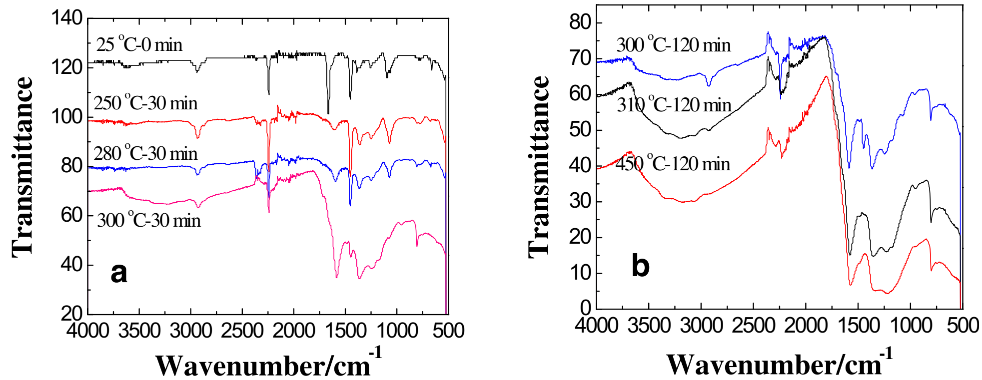

Fig. 6 The FT-IR spectra of nanofibers after different HTT in the range of 25–300 °C for 30 min (**a**) and 300–450 °C for 120 min (**b**)

high enough temperature. Fig. 7 shows Raman spectra of the nanofibers heat treated at various HTT and time. The spectra in the region of Raman shift from 1,000 to 2,000 cm^{-1} are shown in Fig. 7a–e and a full scan Raman spectrum of nanofibers after HTT of 310 °C and time of 120 min is shown in Fig. 7f. Spectra from the sample nanofibers treated under 250 °C and untreated samples at 514.5 nm excitation wavelengths were almost featureless and thus are not been presented here. However, when the HTT is increased to 300 °C, two broad overlapping peaks centered around 1,370 and 1,580 cm^{-1} can be seen clearly, while only one peak at 1,376 cm^{-1} is observed when the HTT is 280 °C and time of 30 min. The higher the treating temperature, the larger and more evident are the peaks. These are the characteristic peaks of D and G bands, which are well known for carbon materials [39], and can be fitted using Gaussian–Lorentzian mixed shape. The line centered near 1,370 cm^{-1} is due to the disordered portion of the carbons since this line is absent in highly oriented pyrolytic graphite, whereas the second line near 1,580 cm^{-1} is

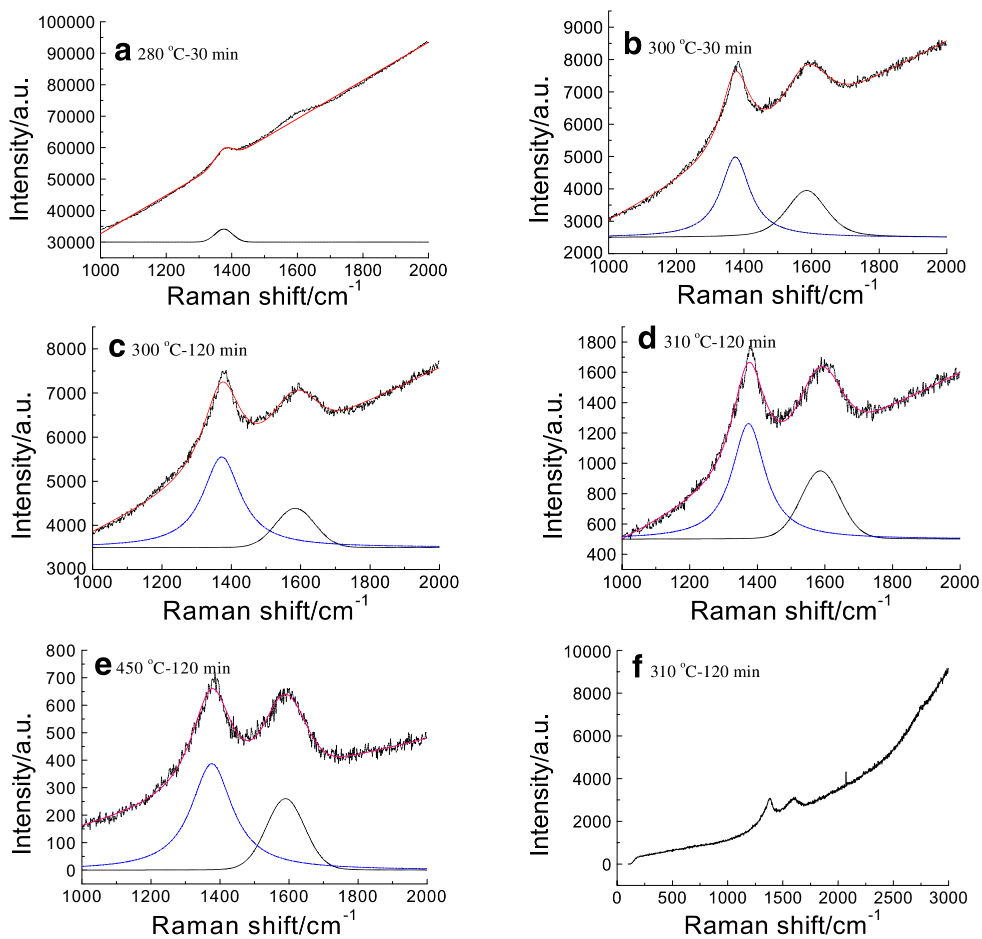

Fig. 7 Raman spectra of the nanofibers pyrolyzed at conditions of various HTT and time. (The *solid lines* are the superposition of the two-fitted Gaussian–Lorentzian lines and the background/noise; the *short dash dot lines* are the single fitted peaks)

indicative of the ordered graphitic crystallites of the resultant carbons. The central positions of D and G bands Raman shift increased slightly with increasing HTT.

The first Raman peak, D band, was initially observed when the HTT reached 280 °C, suggesting that a disordered carbon sheet structure is formed at first. This will partly and increasingly transform into ordered portions of carbon, resulting in the second G peak at higher Raman shift. Furthermore, the G peak becomes higher in height as the HTT and time are increased, and more and more ordered carbon structure has been formed, i.e. the higher the G peak, the higher is the amount of SP^2 (graphite) clusters that exist in the fibers, which will further significantly affect and improve the resulting structure and mechanical properties of the final carbon nanofibers.

Conclusions

Nanofibers with diameter ranging from 220 to 760 nm were obtained by electrospinning of PAN/DMF solution with varying electrospinning conditions, such as solution concentration and applied voltage. The diameters of as-spun fibers increase as the applied voltage is increased, and increase as the concentration of the polymer solution increases.

The oxidative stabilization of PAN precursors during their conversion to carbon fibers is a time-consuming process and plays an important role in determining the final structure and mechanical properties of resultant fibers. The electrospun fibers display very sharp exothermic peak at 297.34 °C. The transition temperature reflected by the most significant structural changes deduced from FT-IR and Raman spectra were closely consistent with the results of DSC and TGA studies.

Acknowledgements We would like to thank HAIPURT (No. 2006KYCX009), the National Natural Science Foundation of Henan (No. 200510465008), and Henan Innovation Project(No. 0523021300) for providing financial support. A part of this work was completed when one of the authors, Wang-xi Zhang, was pursuing his research as a visiting scholar to the University of Manchester, so he would like to thank the help of Professor Young and Ph.D. Eichorn.

References

1. Zhou HJ, Green TB, Joo YL (2006) Polymer 47:7497
2. Saeed K, Park SY, Lee HJ (2006) Polymer 47:8019
3. Maensiri S, Nuansing W, Klinkaewnarong J (2006) J Colloid Interface Sci 297:578
4. Kim GH, Cho YS, Kim WD (2006) Eur Polym J 42:2031
5. Fong H, Chun I, Reneker DH (1999) Polymer 40:4585
6. Ashraf AA, Hamid MAE (2006) Compos Part A Appl Sci Manuf 37:1681
7. Xua CY, Inaic R, Kotakib M, Ramakrishna S (2004) Biomaterials 25:877
8. Li D, Wang Y, Xia Y (2004) Adv Mater 16:361
9. Eugene S, Ulrich B, Ronald D (2005) Polymer 46:2419
10. Yu Z, Borg Y, Chen D (2006) Catal Lett 109:43
11. Yoshimotoa H, Shina YM, Teraia H, Vacanti P (2003) Biomaterials 24:2077
12. Zeng J, Xu X, Chen X (2003) J Control Release 92:227
13. Varaporn P, Pitt S, Ratthapol R, Supawan T (2007) J Polym Res 14:53
14. Kim K, Yen KU, Chang C, Fang D, Benjamin SH (2004) J Control Release 98:47
15. Ramakrishna S, Fujihara K, Teo WE (2006) Materials Today 9:40
16. Wang Y, Serrano S, Santiagiaviles JJ (2002) J Mater Sci Lett 21:1055
17. Hou H, Ge JJ, Zeng J (2005) Chem Mater 17:967
18. Frank K, Yury G, Ashraf A (2003) Adv Mater 15:1161
19. Thandavamoorthy S, Bhat GS, Tock RW (2005) J Appl Polym Sci 96:557
20. Grassie N, McGuchan R (1972) Eur Polym J 18:257
21. Sutasinpromprae J, Jitjaicham S, Nithitanakul M, Meechaisue C, Supaphol P (2006) Polym Int 55:825
22. Kim C, Park SH, Cho JI (2004) J Raman Spectrosc 35:928
23. Wang Y, Serrano S, Jorge J (2003) Synth Met 138:423
24. Zhu D, Koganemaru A, Xu C (2003) J Appl Polym Sci 87:2063
25. Dzenis Y (2004) Science 304:1917
26. Huang ZM, Zhang YZ, Kotaki M (2003) Compos Sci Technol 63:2223
27. Yang W, Yu H, Zhu MF (2006) J Macromol Sci Phys 45:573
28. Deitzel JM, Kleinmer J, Harris D, Tan NCB (2001) Polymer 42:261
29. Kalayci VE, Patra PK, Kim YK, Ugbolue SC, Warner SB (2005) Polymer 46:7191
30. Fennessey SF, Farris RJ (2004) Polymer 45:4217
31. Kedem S, Schmidt J, Paz Y, Cohen Y (2005) Langmuir 21:5600
32. Wang T, Kumar S (2006) J Appl Polym Sci 102:1023
33. Gu SY, Ren J, Vancso GJ (2005) Eur Polym J 41:2559
34. Zhang WX, Liu J, Wu G (2003) Carbon 41:2805
35. Gu SY, Ren J, Wu QL (2005) Synth Met 155:157
36. Bajaj P, Paliwal DK, Gupta AK (1993) J Appl Polym Sci 49:823
37. Hideto K, Kohji T (1997) Polym J 29:557
38. Dalton S, Heatley F, Budd PM (1999) Polymer 40:5531
39. Young RJ, Eichhorn SJ (2007) Polymer 48:2